A Two-Stage Optimal Time-Space Model of Nuclear Radiation Control, Health Protection, and Cost Minimization

Carmen Camacho, Rodolphe Desbordes, Herb Kunze, Davide La Torre

A Two-Stage Optimal Time-Space Model of Nuclear Radiation Control, Health Protection, and Cost Minimization

Carmen Camacho, Rodolphe Desbordes, Herb Kunze, Davide La Torre

November 15, 2023

Abstract

We present a two-stage optimal control model with space and time dimensions to analyze the diffusion of radiations from a nuclear radiation source. The first stage of the model considers the optimal policy to contain the emissions generated from a nuclear radiation source which are diffusing and contaminating the surrounding territories. The second stage, instead, seeks to determine the best location for the nuclear radiation source by minimizing the cost of containment and maximizing the distance from population centers. We illustrate our approach through different numerical examples and we also provide a real case study by using available data from Chernobyl.

Nuclear Energy Health protection Diffusion

JEL Classification: C60, Q4, I10

1 Introduction

Despite the huge consequences caused by the 2011 Fukushima nuclear disaster in Japan—which is considered the most severe nuclear accident after Chernobyl—many nations reiterated their intent to invest in nuclear energy. The recent energy crisis and the political instability in certain regions have also contributed to the revitalization of the debate on alternative sources of energies, in particular nuclear energy. This has also stimulated the debate around the chances of nuclear accidents, and the prevention, mitigation, and management of such critical scenarios. Several international organizations, agencies, committees, and working groups (for instance the NEA Working Group on the Analysis and Management of Accidents (WGAMA), International Atomic Energy Agency (IAEA), the European Commission (EU), and others) conduct regular meetings to assess and enhance the technical basis needed to prevent, mitigate and manage potential accidental situations in nuclear power plants. Today there are about 440 nuclear power reactors operating in 32 countries plus Taiwan, with a combined capacity of about 390 GWe. In 2021 these provided 2653 TWh, about 10% of the world's electricity (see Figure 1). On top of this, nuclear power capacity worldwide is increasing steadily, with about 60 power reactors under construction in 15 countries, notably China, India and Russia. Units whose construction is currently suspended, i.e. Ohma 1 and Shimane 3 (Japan), and Khmelnitski 3 and 4 (Ukraine), do not show in Figure 1. Most reactors on order or planned are in Asia, though there are major plans for new units in Russia. There are also consistent worldwide investments in plant upgrading to create further capacity.

Our paper wishes to contribute to the ongoing debate on how to balance safety, cost minimization and radiation exposure, by introducing a two-stage optimal control model with time and space variables to optimally choose the location of a new nuclear radiation source in a given region. Thanks to the specific form of the optimal control model we are able to determine the closed-form expression of the optimal cost for certain families of source functions. This allows to determine the best location in a second stage: We solve a static optimization model in which the objective function is expressed as a convex combination of optimal cost and distance from population centres. Again, for certain family of source expressions, we can provide the exact closed-form expression of the optimal plant location.

The paper is organized as follows. Section 2 presents a brief literature review of the current debate on preventing, mitigating and management of potential accidents in nuclear plants. Section 3 presents the pure dynamic model and provides some numerical illustration of the long-run behaviour. Section 4 presents a parameter estimation procedure based on the solution of an inverse problem and an interesting case study using data from the Ukranian territory surrounding the Chernobyl nuclear

Figure 1: Nuclear Power Reactors under Construction (source www.world-nuclear.org)

Power reactors under construction

Start †		Reactor	Model	Gross MWe
2023	Bangladesh	Rooppur 1	VVER-1200	1200
2023	China, CNNC	Xiapu 1	CFR600	600
2023	Korea, KHNP	Shin Hanul 2	APR1400	1400
2023	Korea, KHNP	Saeul 3	APR1400	1400
2023	Turkey	Akkuyu 1	VVER-1200	1200
2023	UAE, ENEC	Barakah 4	APR1400	1400
2023	USA, Southern	Vogtle 4	AP1000	1250
2024	Bangladesh	Rooppur 2	VVER-1200	1200
2024	China, CGN	Fangchenggang 4	Hualong One	1180
2024	China, Guodian & CNNC	Zhangzhou 1	Hualong One	1212
2024	China, SPIC & Huaneng	Shidaowan 1	CAP1400	1500
2024	France, EDF	Flamanville 3	EPR	1650
2024	India, NPCIL	Kakrapar 4	PHWR-700	700
2024	India, NPCIL	Kalpakkam PFBR	FBR	500
2024	Iran	Bushehr 2	VVER-1000	1057
2024	Korea, KHNP	Saeul 4	APR1400	1400
2024	Slovakia, SE	Mochovce 4	VVER-440	471
2024	Turkey	Akkuyu 2	VVER-1200	1200
2025	China, CGN	Taipingling 1	Hualong One	1200
2025	China, Guodian & CNNC	Zhangzhou 2	Hualong One	1212
2025	China, SPIC & Huaneng	Shidaowan 2	CAP1400	1500
2025	India, NPCIL	Kudankulam 3	VVER-1000	1000
2025	India, NPCIL	Kudankulam 4	VVER-1000	1000
2025	Russia, Rosenergoatom	Kursk II-1	VVER-TOI	1255
2025	Russia, Rosenergoatom	Kursk II-2	VVER-TOI	1255
2025	Turkey	Akkuyu 3	VVER-1200	1200
2026	China, CGN	Cangnan/Sanao 1	Hualong One	1150
2026	China, CGN	Taipingling 2	Hualong One	1202
2026	China, CNNC	Changjiang SMR 1	ACP100	125
2026	China, CNNC	Tianwan 7	VVER-1200	1200
2026	China, CNNC	Xiapu 2	CFR600	600
2026	China, Huaneng & CNNC	Changjiang 3	Hualong One	1200
2026	India, NPCIL	Rajasthan 7	PHWR-700	700
2026	India, NPCIL	Rajasthan 8	PHWR-700	700
2026	Russia, Rosatom	BREST-OD-300	BREST-300	300
2026	Turkey	Akkuyu 4	VVER-1200	1200

2027	Argentina, CNEA	Carem	Carem25	29
2027	China, CGN	Cangnan/Sanao 2	Hualong One	1150
2027	China, CNNC	Sanmen 3	CAP1000	1250
2027	China, CNNC	Tianwan 8	VVER-1200	1200
2027	China, CNNC & Datang	Xudabao 3	VVER-1200	1200
2027	China, Huaneng & CNNC	Changjiang 4	Hualong One	1200
2027	China, SPIC	Haiyang 3	CAP1000	1250
2027	China, SPIC	Haiyang 4	CAP1000	1250
2027	India, NPCIL	Kudankulam 5	VVER-1000	1000
2027	India, NPCIL	Kudankulam 6	VVER-1000	1000
2027	UK, EDF	Hinkley Point C1	EPR	1720
2028	Brazil, Eletrobrás	Angra 3	Pre-Konvoi	1405
2028	China, CGN	Lufeng 5	Hualong One	1200
2028	China, CNNC	Sanmen 4	CAP1000	1250
2028	China, CNNC & Datang	Xudabao 4	VVER-1200	1200
2028	Egypt, NPPA	El Dabaa 1	VVER-1200	1200
2028	UK, EDF	Hinkley Point C2	EPR	1720
2030	Egypt, NPPA	El Dabaa 2	VVER-1200	1200
2030	Egypt, NPPA	El Dabaa 3	VVER-1200	1200

plant. Section 5 presents the main optimization model and discusses the optimality conditions for the two stage problem. Finally Section 6 concludes.

2 Literature Review

Although the 2011 Fukushima nuclear accident in Japan initially decreased public acceptance of nuclear energy [KKK13], leading some countries (e.g. Germany, Italy, Switzerland) to exclude the latter from their energy mix, the imperative to curb climate change has rekindled interest in this low-carbon source of energy. In 2023, according to the World Nuclear Association,[1] 436 reactors are in operation in 31 countries, 59 are under construction, 100 are planned, and 323 are proposed. However, for nuclear energy to curb carbon emissions, thousands more would need to be rapidly built by the end of this century [KE07].

A higher number of operating nuclear reactors is likely to mean a higher frequency of nuclear accidents in the future. [RS16] and [Eng20] estimate that, given an observed failure rate of 1 in 3706 reactor-years in any single reactor and the current number of nuclear reactors, the chance of a major nuclear accident in the near future may be already larger than 70%.

Finding an optimal location for a new nuclear radiation source is thus a crucial issue for policy-makers. From a safety perspective, the fundamental goal is to protect people and the environment from the harmful effects of ionising radiation [IAE15].

This implies that suitability of the site depends on whether the nuclear reactor integrity could be compromised by external natural (e.g. earthquake) or human-induced events (e.g. chemical plants nearby) and whether the characteristics of the site could facilitate the transfer of radiation to surrounding areas due to high air or water dispersion, large population density, and difficulties to implement any emergency plan such as population evacuation. [DM17] and [MY21] emphasise that the societal impacts (e.g. cost of land contamination, loss of industrial production and electricity capacity, population relocation) may be much larger, including in terms of indirectly related deaths, than immediate

[1] https://world-nuclear.org/information-library/facts-and-figures/world-nuclear-power-reactors-and-uranium-requireme.aspx

direct individual health risks. In the context of the Fukushima accident, evacuation of elderly people and the rise in electricity prices have had much larger effects on mortality than the low levels of radiation exposure [HOM+16, NUV21, UNS22].

Technical and economic considerations also play a role, such as the availability of cooling water, access to an electrical grid, and the eventual impact on tourism. The high number of, sometimes conflicting, factors that needs to be taken into account in the 'best' choice problem implies that a form of multi-criteria decision making (MCDM) is frequently applied; [AUY23] provide a review of this literature.

In this paper, we revisit the issue of the best location of a nuclear radiation source in a two-stage optimal control model. Radionuclide pollution involves spatial diffusion and radioactive decay. Atmospheric dispersion is based on Fick's law and is fully compatible with the Gaussian plume diffusion model traditionally assumed in the nuclear safety literature [Pet20]. Ground concentration usually falls with distance, although the shape of the relationship strongly depends on atmospheric conditions and height of release. Isotopes vary in their half-life (the time it takes for half of the isotope to decay to something else). For two major radioactive fission products, largely released in the atmosphere after the Chernobyl and Fukushima accidents, iodine (131^I) and cesium (137^{Cs}), it is respectively about 8 days and 30 years [KYS14, AEM+15]. To estimate representative values of our key parameters, we rely on Chernobyl data.[2] Given the possibility of radionuclide pollution in case of a nuclear accident, the policymaker must determine the best location, by attempting to minimise both the cost of containing nuclear radiations and the number of exposed people to radiation. An inherent trade-off exists. For example, locating a nuclear plant from far-distant cities reduces the risk of radiation but increases infrastructure costs. Likewise, depending on the acceptable radiation dose, especially when considering societal risks [MOT+15, TS16], nuclear plants could be located closer to population centres. [Mub95] illustrates such a trade-off: the lower the allowable level of long-term exposure, the smaller early fatality and latent fatality costs ('the number of exposed people to radiation') but the larger the off-site protective action costs ('the costs of containing nuclear radiations', e.g. the costs of emergency actions, cleanup and interdiction of contaminated land and structures, long-term relocation of people.) Hence, it may be optimal from a cost perspective, to allow for a higher long-term interdiction limit. There is an intense debate about the maximum permissible dose. For example, doubts have been cast regarding the validity of the linear no-threshold (LNT) model, which states that any ionising radiation may induce stochastic health effects (e.g. a cancer) whatever the dose level and that it is the cumulative dose that matters and not the dose rate [FGMF12, SMS16, MAC+17, FC18]. Rejecting the LNT at low dose would lead to a substantial revision upward (by a factor of 50) of the radiation level for evacuation [Cut12].

3 The Diffusion Model

In the sequel let us denote by $R_{y_P}(x,t)$ the level of radiation at a certain location x and time t when there is a nuclear radiation source at y_P. For technical reasons, we suppose that R_{y_P} is a C^1 function in time and C^2 and integrable in space, that is $R_{y_P} \in C^{2,1}(\mathbb{R}\times\mathbb{R}) \cap L^1(\mathbb{R}\times\mathbb{R})$. The diffusion equation, based on Fick's law that states that neutrons diffuse from high concentration to low concentration, provides an analytical solution of spatial neutron flux distribution and it takes the form:

$$\begin{cases} \frac{\partial R_{y_P}(x,t)}{\partial t} = d_1 \frac{\partial^2 R_{y_P}(x,t)}{\partial x^2} + d_2 R_{y_P}(x,t) + d_3 \int_{\mathbb{R}} \phi(x-\omega) R_{y_P}(\omega,t) d\omega + [1-\theta(x,t)] S(y_P,t), \\ \lim_{x\to\pm\infty} \frac{\partial R_{y_P}(x,t)}{\partial x} = 0, \\ R_{y_P}(x,0) = R_{y_P,0}(x) = R_0(x), \end{cases} \tag{1}$$

In this equation we have modelled two different forms of diffusion: a classical one, based on the notion of the Laplacian, and an integral one which models the slow diffusion of heavy pollutants. The integral term is a weighted average of radiations from x's perspective, where the level of radiations at each location ω is weighted by a function ϕ, which one could interpret as a kind of measure. ϕ is a real

[2] Using existing data about Chernobyl emissions and a global model of the atmosphere, [LKL12] estimate the global risk of radioactive contamination if a major nuclear accident occurs.

function of space such that

$$\int_{\mathbb{R}} \phi(\omega)d\omega = 1.$$

The function ϕ characterizes the global extent of nuclear radiations. From a technical point of view, we assume that ϕ takes a Gaussian distribution defined as $\phi(x) = \frac{1}{\sqrt{2\pi\sigma^2}} e^{-\frac{(x-\mu)^2}{2\sigma^2}}$, where $\mu \in \mathbb{R}$ and $\sigma > 0$.

The term $S(y_P, t)$ models the source of emissions at the location y_P while the term $d_2 R_{y_P}(x,t)$ describes the natural radiation decay rate $d_2 < 0$. At this stage the term $\theta(x,t)$ is exogenous and it describes the local effort to put in place at x and at the time t in order to limit the spread of radiation from the nuclear site at y_P. Finally, $R_0(x)$ is the initial distribution of radiation, which is independent of the location site y_p. The initial distribution of radiation over space $R_0 : \mathbb{R} \longrightarrow \mathbb{R}^+$, is a strictly positive function in $C^2(\mathbb{R}) \cap L(\mathbb{R})$ where $C^2(\mathbb{R})$ is the space of twice differentiable functions on $\mathbb{R}$ and $L(\mathbb{R})$ is the set of all integrable functions over $\mathbb{R}$.

Under these hypotheses, the theory of parabolic equations ensures that the above boundary value problem Eq. (1) admits a unique classical solution [Lie]. Moreover, the strong maximum principle for parabolic equations guarantees that R_{y_P} is nonnegative for all $x \in \mathbb{R}$ and $t > 0$ [PW12].

Let us define average radiation $\bar{R}_{y_P}$, as the average of the radiation term $\overline{R}_{y_P}(t)$ over $\mathbb{R}$, that is

$$\bar{R}_{y_P}(t) = \int_{\mathbb{R}} R_{y_P}(x,t)dx \tag{2}$$

and let us assume that $\theta(\cdot, t) \in L(\mathbb{R})$ for any fixed $t \in \mathbb{R}$. Then, integrating equation (1) over $\mathbb{R}$ we obtain that:

$$\begin{cases} \frac{d\bar{R}_{y_P}(t)}{dt} = (d_2 + d_3)\bar{R}_{y_P}(t) + (1 - \bar{\theta}(t))S(y_p, t), \\ \bar{R}_{y_P}(0) = \int_{\mathbb{R}} R_{y_P,0}(x)dx, \end{cases}$$

where

$$\bar{\theta}(t) = \int_{\mathbb{R}} \theta(x,t)dx \tag{3}$$

which is finite thanks to the integrability assumption of $\theta(\cdot, t)$.

Proposition 1. *Suppose that $\bar{\theta}(t) \in [0,1]$ for any $t \geq 0$, $\sup_{s\in\mathbb{R}}(1 - \bar{\theta}(s))S(y_p, s) \leq M$ and that $d_2 + d_3 < 0$. Then any trace of radiation $\bar{R}_{y_P}(t)$ will disappear in finite time.*

Example 3.1. *In this example we illustrate the workings of diffusion and emissions showing the behavior of the model under different assumptions on emissions and different parameters' combinations. In particular, the simulations have been run with different values of d_i and source on or off. For the unit time interval, all graphs fit inside the spatial domain $[-20, 20]$. The initial condition R_0 takes the form of:*

$$R_0(x) = 0.3e^{(-0.1(x+7)^2)} + 0.8e^{(-0.2(x-5)^2)}$$

Note that R_0 includes two peaks of different intensity at $x = -7$ and $x = 5$. So we are purposely setting two initially highly polluted zones around each of these peaks, which are not in the geographical center and which are distant to the borders. Worth observing, the region between the two peaks is more polluted than distant locations, receiving emissions from both zones.

In the simulations, we have used the following aggregator function

$$\phi(x) = \frac{1}{\sqrt{\pi}} e^{-x^2}$$

in which $\mu = 0$ and $2\sigma^2 = 1$.

Let us next study the role of each of the elements in the diffusion process. According to (1), the dynamic behavior of radiations depends on the one hand on the current level of radiations and on two very different types of diffusion, local and global diffusion, whose strength is measured by d_1 in the case of local diffusion and by d_3 in the global. Very importantly at this point, remark how the global effect will be the intertwined result of how the whole of local emissions aggregate via function ϕ to form an aggregate emission measure, and its strength. Next, we propose three exercises in which we will sequentially study each of the leading diffusion factors. Our first exercise assumes that the pure

diffusion component is deactivated ($d_1 = 0$) and that there is no radiation source ($S \equiv 0$). Worth underlining, this case is equivalent to studying a continuum of independent locations with no link nor economic nor environmental. Figure 2 shows the evolution of the level of radiations over space and time when $d_2 = 5$. The high value of d_2 implies that current radiations will drive the accumulation process in time. Note how in this case, the level of radiations increase at all locations with time due to self-reinforcement, and the two initial peaks gain force evolving independently due to the absence of diffusion.

In the exercise depicted in Figure 3 we add a pure diffusion term with a non-zero level of diffusion ($d_1 = 5$) and still no source ($S \equiv 0$). In this case the effect of diffusion can be greatly appreciated. Indeed, note how the two peaks merge with time in a unique bell.

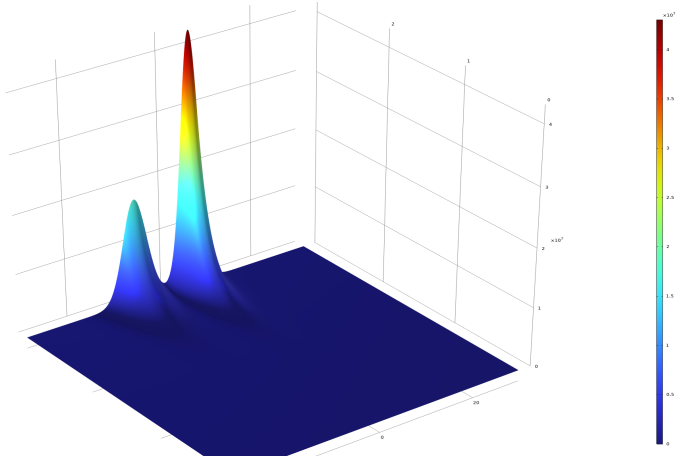

Figure 2: Numerical results with $d_1 = 0$, $d_2 = 5$, $d_3 = 1$

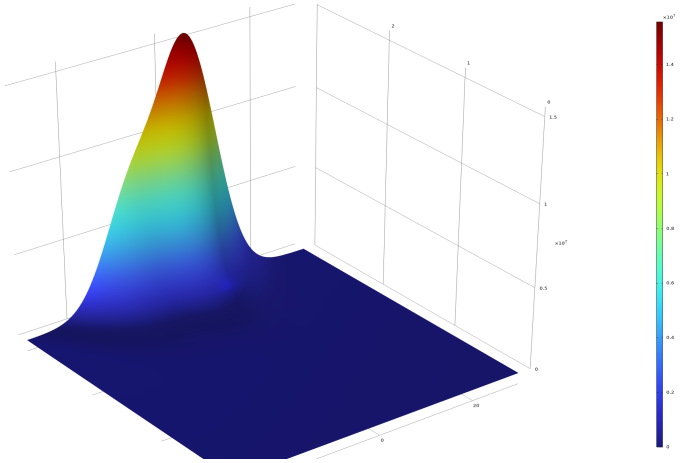

Figure 3: Numerical results with $d_1 = 5$, $d_2 = 5$, $d_3 = 1$

Finally in the last numerical simulation we assume the presence of both a local diffusion effect and a global effect, plus a radiation source at $x = 0$, the geographical center. The emissions' source lies between the two initially most polluted areas. We assume $\theta = \frac{1}{2}$, $y_p = 0$, and $S(0,t) = 2.5(2+\cos(\pi t))$ so that emissions come as waves in time. Under this assumption, the amount of new emissions from $x = 0$ oscillate between 5 and 7.5. We have also used $d_1 = d_2 = d_3 = 1$, changing the values of d_1 and d_2 with respect to the two previous exercises so as to obtain a slower and more illustrative process. Results are presented in Figure 4. The presence of a pure diffusion term, $d_1 \neq 0$, induces the spread of the radiation wave across space and time while the injection of new contaminant through the radiation source modifies the intensity of the radiation effect. Under our assumptions, the two peaks shape is

preserved throughout the entire time period.

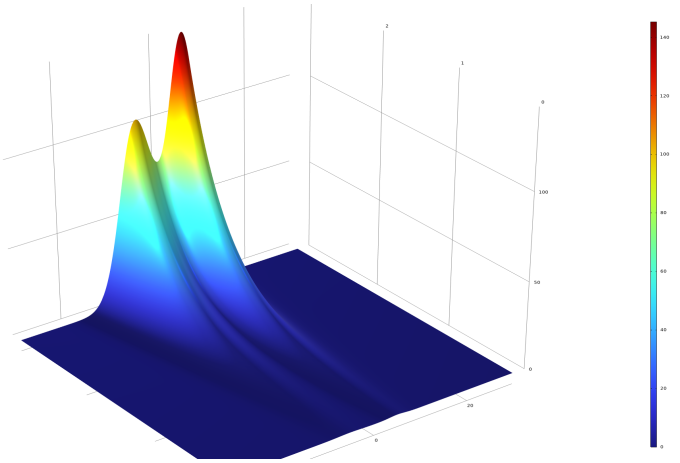

Figure 4: Numerical results of the model with source

4 Model Parameter Estimation using Inverse Problems

Suppose that there are available data on radiation in a given region, and that we would like to interpolate them to generate an estimated function $\hat{R}_{y_P}(x,t)$. One way to interpolate the available data to get $\hat{R}_{y_P}(x,t)$ consists in using an orthonormal Fourier basis $\{\psi_j\}_{j\in\mathbb{N}}$ of $L^2(\mathbb{R})$ such that $\lim_{x\to\pm\infty}\frac{\partial\psi_j}{\partial x}=0$. Therefore we use the available data to approximate the following integrals which represent the projections of $\hat{R}_{y_P}(x,t)$ over the Fourier basis:

$$a_j(t)=\int_{\mathbb{R}}\hat{R}_{y_P}(x,t)\psi_j(x)dx \tag{4}$$

so that $\hat{R}_{y_P}(x,t)$ can be represented in terms of its Fourier components as follows:

$$\hat{R}_{y_P}(x,t)=\sum_{j\geq 0}a_j(t)\psi_j(x) \tag{5}$$

Let us also suppose that both the source $S(y_P,t)$ and the effort $\theta(x,t)$ are known. We aim at estimating the parameters d_1, d_2, and d_3 by solving an inverse problem for the boundary value problem. If we define the distance function

$$\Delta(d_1,d_2,d_3)=\left\|\frac{\partial\hat{R}_{y_P}}{\partial t}-d_1\frac{\partial^2\hat{R}}{\partial x^2}-d_2\hat{R}-d_3\int_{\mathbb{R}}\phi(x-\omega)\hat{R}d\omega-[1-\theta]S\right\|_{L^2}^2 \tag{6}$$

Once a guess for ϕ has been decided, all terms included in the norm are known except the three parameters d_1, d_2, and d_3. Let us observe that the expression in the norm is a function of space and time and, therefore, the L^2 norm is intended with respect to both these components.

The function Δ is a function of the unknown parameters d_1, d_2, and d_3 is reduced to the following minimization problem:

$$\min_{\mathbf{d}}\Delta(\mathbf{d})+\nu\|\mathbf{d}\| \tag{7}$$

subject to

$$\begin{cases} d_1,d_3\geq 0 \\ d_2\leq 0 \end{cases}$$

where $\mathbf{d}$ is a vector whose components are d_1, d_2, and d_3, $\|\cdot\|$ is the Euclidean norm, and ν is a Tikhonov's regularization term. Inverse problems for PDEs have been widely investigated in the

literature. The inverse problem is the opposite of the direct problem: rather than studying the analytical and numerical properties of the solution to a PDE equation, the inverse problem starts from an empirical observation of the solution and tries to estimate the values of the unknown model parameters. The goal is to determine a set of parameters which generate a PDE solution as much as possible close to—in some norm—the empirical observations and information about the solution. In general an inverse problem is ill-posed. For more details on this discussion one can read [K+11, Tik63, Vog02].

4.1 A Case Study: The Case of Chernobyl

Chernobyl provides a case study for data deficiency in the environmental protection framework of the International Commission on Radiological Protection [BBG+20]. Several studies have been conducted to measure the impact of radionuclide concentration and absorbed dose rate in wildlife and soil samples [BGB+09, BBG+20, KLZ+18, KLZ+20]). For our analysis, we use the Chernobyl radiation dataset ([KLZ+17]). This dataset was developed to enable data collected between May 1986 and 2014 by the Ukrainian Institute of Agricultural Radiology (UIAR) after the Chernobyl accident to be made publicly available. The dataset includes results from comprehensive soil sampling across the Chernobyl Exclusion Zone (CEZ, see Figure 5). It provides measurements of the 137Cs isotope at various latitudes and longitudes on various days. We convert the location information into a single variable x corresponding to the distance from the Chernobyl nuclear power plant in order to model the spread of radiation using our model, with the assumption that the spread depends only on radius. With this assumption, we can reflect the data through the origin to get a dataset on $\mathbb{R}$. The data are plotted in Figure 6.

Figure 5: Chernobyl Exclusion Zone

Fitting R_{y_P} to the data (see Figure 7) and assuming a negative squared exponential form in space, we get that a good fitting is provided by the following function

$$R_{y_P}(x,t) = 53946.95356 e^{-0.87476t} e^{-0.03512x^2} \tag{8}$$

We now try to solve an inverse problem for the equation

$$\begin{cases} \frac{\partial R_{y_P}(x,t)}{\partial t} = d_1 \frac{\partial^2 R_{y_P}(x,t)}{\partial x^2} + d_2 R_{y_P}(x,t) + d_3 \int_{\mathbb{R}} \phi(x-\omega) R_{y_P}(\omega,t) d\omega, \\ \lim_{x\to\pm\infty} \frac{\partial R_{y_P}(x,t)}{\partial x} = 0, \\ R_{y_P}(x,0) = R_{y_P,0}(x) \end{cases} \tag{9}$$

in order to determine an estimation of the unknown parameters d_1, d_2, and d_3. Clearly $R_{y_P}(x,t)$ satisfies the initial and boundary conditions. Let us also observe that if we plug the above interpolated

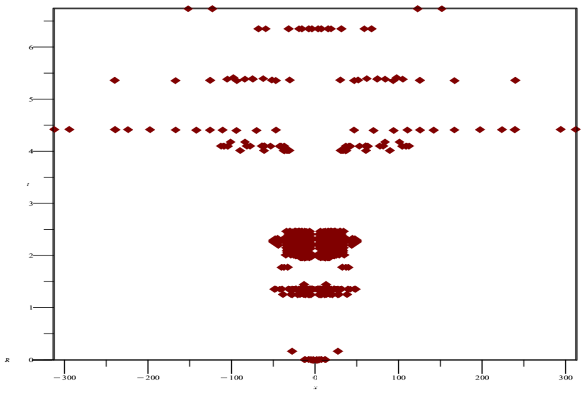

Figure 6: 2D data representation

function $R_{y_P}(x,t)$ into the above PDE, we can reduce the PDE to the following ODE:

$$\begin{cases} d_1 \frac{\partial^2 f(x)}{\partial x^2} + (d_2 + a) f(x) + d_3 \int_{\mathbb{R}} \phi(x-\omega) f(\omega) d\omega = 0, \\ \lim_{x \to \pm\infty} f'(x) = 0, \\ f(x) = R_{y_P,0}(x), \end{cases}$$

where the expressions of a and $f(x)$ are known and equal to -0.87476 and $53946.95358e^{-0.035116x^2}$, respectively. By minimizing the distance between the left hand side and zero, we have have the following results: $d_1 = 0$, $d_2 = -0.12524$, $d_3 = 1$ and

$$\phi(x-\omega) = 2839.63759e^{-5033.12658(x-\omega)^2}.$$

We actually presupposed that ϕ was Gaussian, and, more, that it was such that the exponents combined in a helpful way.

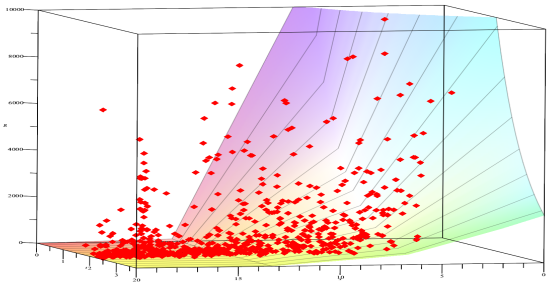

Figure 7: 3D data representation

5 The Main Result: A Two-Stage Optimal Control Model

We suppose to have an infinite one-dimensional domain in space and we focus on a fixed horizon time window $[0,T]$. We propose a two-step time-space model to decide on the optimal location of a nuclear waste while, at the same time, minimizing the spread of nuclear radiations and the level of irradiated people. Our model involves two steps, and it reads as follows. Let $y_P \in \Omega$, the position of the nuclear waste site to be determined in an optimal way. Let Ω be a compact subset of $\mathbb{R}$. Let $y_p \in \Omega$ be a

given location representing a city, farm, and any other location affected by radiation contamination (and potentially the next host of a nuclear facility). We denote by $R_{y_P}(x,t)$ the level radiations at the position x as a consequence of installation of nuclear waste at location $y_P \in \Omega$. For any fixed location y_P by exerting an effort θ at each location and moment in time- to be determined in an optimal way at the second step of the optimization process - the decision maker wishes to minimize the effort to contain the emission of nuclear radiations from y_P while minimizing the total number of irradiated people at the final horizon T.

STEP 1: For any fixed $y_P \in \Omega$, the model reads as:

$$J(y_P) = \min_{\theta} \int_0^T \int_{\mathbb{R}} \theta^2(x,t) e^{-\rho t} dx dt + \chi e^{-\rho T} \int_{\mathbb{R}} R_{y_P}(x,T) g(x) dx, \tag{10}$$

subject to

$$\begin{cases} \frac{\partial R_{y_P}(x,t)}{\partial t} = d_1 \frac{\partial^2 R_{y_P}(x,t)}{\partial x^2} + d_2 R_{y_P}(x,t) + d_3 \int_{\mathbb{R}} \phi(x-\omega) R_{y_P}(\omega,t) d\omega + [1-\theta(x,t)] S(y_P,t), \\ \lim_{x \to \pm\infty} \frac{\partial R_{y_P}(x,t)}{\partial x} = 0, \\ R_{y_P}(x,0) = R_{y_P,0}(x), \\ 0 \leq \theta(x,t) \leq 1, \end{cases}$$

where:

- $R_{y_P}(x,t)$ is a state variable and it measures the level of radiations at a given location x and time t once the nuclear waste has been deposited at location y_P;
- $\theta(x,t)$ is a control variable and it describes the local effort to put in place at x at time t in order to limit the spread of radiations from the nuclear site at y_P;
- $g(x)$ is the weight that the policy maker attaches to location x. Note that g could be the location's population density, natural or economic value, etc. Note that g can also be the product of a population density function and a location dependent treatment cost function.

The objective function

$$\int_0^T \int_{\mathbb{R}} \theta^2(x,t) e^{-\rho t} dx dt + \chi e^{-\rho T} \int_{\mathbb{R}} R_{y_P}(x,T) g(x) dx, \tag{11}$$

is composed by two terms. The first term measures the cost of efforts to put in place to limit the spread of radiations from the nuclear site, to be minimized. The second one measures total weighted radiations at the final horizon, to be minimized. This term could be interpreted as a proxy for the level of irradiated people and in this regard, this second term could be linked to the health cost to deliver treatment to contaminated people at the final horizon T. Hence, χ is to be understood as a (relative) penalty for total radiations or as a measure of treatment costs (if they were spatially homogeneous).

The dynamic constraint:

$$\frac{\partial R_{y_P}(x,t)}{\partial t} = d_1 \frac{\partial^2 R_{y_P}(x,t)}{\partial x^2} + d_2 R_{y_P}(x,t) + d_3 \int_{\mathbb{R}} \phi(x-\omega) R_{y_P}(\omega,t) d\omega + [1-\theta(x,t)] S(y_P,t) \tag{12}$$

takes the form of a reaction-diffusion equation with four different terms on the right hand side: the first one is a pure local diffusion expression, the second one models the radiation growth, the third term is a global diffusion term, while the last one is a source of nuclear radiation generated at the nuclear waste site. The expression of $S(y_P,t)$ is a known term.

STEP 2: Once the expression of $J(y_P)$ is known, the decision maker wishes to minimize in the second step the total distance to the waste location while minimizing overall cost and containing total radiations below a threshold $\bar{R}$, that is

$$\max_{y_P \in \Omega} \alpha_1 \int_{\Omega} (y_P - y_i)^2 dF(i) - \alpha_2 J(y_P) \tag{13}$$

subject to

$$\int_{\mathbb{R}} R_{y_P}(x,T)g(x)dx \leq \bar{R}, \tag{14}$$

with $\alpha_1, \alpha_2 \geq 0$. Also in this case the objective function is a weighted combination of two terms: The first one measures the distance from the nuclear waste site to populated areas, to be maximized. The second one, instead, is the optimal cost whose expression is determined at STEP 1. Worth noting, function F in (13) is different from g, so that the policy maker could introduce some additional geographical or strategical information to her decision problem.

5.1 First step

We address the problem of maximizing (11) subject to (12) by restricting our analysis to sufficiently regular functions defined on the space $C^{2,1}(\mathbb{R}\times(0,T))\cap L(\mathbb{R}\times[0,T])$, where $C^{2,1}(\mathbb{R}\times(0,T))$ is the function space defined as the class of functions which are twice continuously differentiable with respect to the first variable and continuously differentiable with respect to the second variable. Working in $C^{2,1}(\mathbb{R}\times(0,T))\cap L(\mathbb{R}\times[0,T])$ allows the use of standard techniques in Optimal Control and to invoke classical results.

Definition 5.1. *A trajectory $[\theta(x,t), R_{y_p}(x,t)]$, with i in $C^{2,1}(\mathbb{R}\times(0,T))\cap L(\mathbb{R}\times[0,T])$ and θ piecewise-$C^{2,1}(\mathbb{R}\times(0,T))\cap L(\mathbb{R}\times[0,T])$, is admissible if R_{y_p} is a solution to problem (12) with control θ on $\mathbb{R}\times[0,T]$, if the integral objective function (11) converges.*

A trajectory $[\theta^*(x,t), R^*_{y_p}(x,t)]$ for $t\in[0,T]$, $x\in\mathbb{R}$, is an optimal solution of problem (11) subject to (12) if it is admissible and if it is optimal in the set of admissible trajectories; that is, for any other admissible trajectory $[\theta(x,t), R_{y_p}(x,t)]$, the value of the integral (11) is not greater than its value corresponding to $[\theta^*(x,t), R^*_{y_p}(x,t)]$.

Invoking Ekeland's method of variations as in Raymond and Zidani (1999), we obtain the Pontryagin optimality conditions as stated in the following result:

Theorem 1. *Under the model hypotheses, the set of optimal necessary conditions which describe the interior optimal solution to problem (11) subject to (12) is given by*

$$I\begin{cases}
\frac{\partial R_{y_P}(x,t)}{\partial t} = d_1\frac{\partial^2 R_{y_P}(x,t)}{\partial x^2} + d_2 R_{y_P}(x,t) + d_3\int_{\mathbb{R}}\phi(x-\omega)R_{y_P}(\omega,t)d\omega + [1-\theta(x,t)]S(y_P,t),\\
\frac{\partial \mu_1(x,t)}{\partial t} + d_1\frac{\partial^2\mu_1(x,t)}{\partial x^2} + (d_2-\rho)\mu_1(x,t) + d_3\int_{\mathbb{R}}\phi(\omega-x)\mu_1(\omega,t)d\omega + \mu_4(x,t) = 0,\\
2\theta(x,t) - \mu_1(x,t)S(y_P,t) + \mu_2(x,t) - \mu_3(x,t) = 0,\\
\lim_{x\to\pm\infty}\frac{\partial R_{y_P}(x,t)}{\partial x} = 0,\\
\lim_{x\to\pm\infty}\frac{\partial \mu_1(x,t)}{\partial x} = 0,\\
\mu_i(x,t)\geq 0,\\
\mu_1(x,T) = \chi g(x),\\
\mu_2(x,t)\theta(x,t) = 0,\\
\mu_3(x,t)\left[1-\theta(x,t)\right] = 0,\\
\mu_4(x,t)R_{y_P}(x,t) = 0,\\
R_{y_P}(x,0) = R_0(x),\\
0\leq\theta(x,t)\leq 1,\\
R_{y_P}(x,t)\geq 0.
\end{cases}$$

where the co-state variable μ_1 is piecewise $C^{2,1}(\mathbb{R}\times(0,T))\cap L(\mathbb{R}\times[0,T])$, and μ_2,μ_3,μ_4 are piecewise $C(\mathbb{R}\times[0,T])\cap L(\mathbb{R}\times[0,T])$.

It is worth noting that along the interior solution $2\theta(x,t) = \mu_1(x,t)S(y_P,t)$, and μ_1 obtains independently of R_{y_P}.

Proof. See Appendix 7.2. ■

Next, we will restrict the class of aggregator functions g that will enable the obtaining of an explicit and separable trajectory for the interior solution for μ_1 and for an aggregate measure of radiations.

Proposition 2. *Under the model hypothesis, there exists a separable solution for the co-state variable* $\mu_1(x,t)$, $\mu_1(x,t) = f(t)g(x)$ *with* $f(T) = \chi$. *In particular, if function* f *is given by*

$$f(t) = \chi e^{\varphi(T-t)},$$

for some $\varphi \in \mathbb{R}$, *then* g *solves*

$$d_1 g_{xx}(x) + (d_2 + \varphi - \rho)g(x) + d_3 \int_{\mathbb{R}} \phi(\omega - x)g(\omega)d\omega = 0.$$

Proof. See Appendix 7.3. ■

We can refine our solution further under the following assumption:

Assumption 1. *There exist constants* h_1 *and* h_3 *such that*

$$g_{xx}(x) = h_1 g(x), \tag{15}$$

$$\int_{\mathbb{R}} \phi(\omega - x)g(\omega)d\omega = h_3 g(x), \tag{16}$$

for all x. *Besides, function* g *satisfies that* $\lim_{x\to\pm\infty} g'(x) = 0$.

Corollary 1. *Under the model hypothesis and Assumption 1, there exists a separable solution for the co-state variable* $\mu_1(x,t)$, $\mu_1(x,t) = f(t)g(x)$ *with*

$$f(t) = \chi e^{(d_1 h_1 + d_2 + d_3 h_3 - \rho)(T-t)}.$$

In this case $\mu_1(x,t)$ *obtains*

$$\mu_1(x,t) = \chi g(x) e^{(d_1 h_1 + d_2 + d_3 h_3 - \rho)(T-t)}. \tag{17}$$

Proof. See Appendix 7.7. ■

Using the value for μ_1 in (17), optimal effort trivially obtains using that along the optimal solution $2\theta(x,t) = \mu_1(x,t)S(y_P,t)$:

$$\theta(x,t) = \frac{\chi}{2} g(x) S(y_P,t) e^{(d_1 h_1 + d_2 + d_3 h_3 - \rho)(T-t)}.$$

The particular solution for μ_1 in Corollary 1 is immensely useful. Under Assumption 1, not only can we obtain the optimal effort to exert at each location to contain radiations, but we also can compute the value of the objective function as we show next. Only then will the policy maker be able to compare all different locations and choose one to implement the nuclear facility.

Substituting the optimal solution for θ, we can write the objective function as

$$\frac{1}{4}\int_0^T S^2(y_P,t) f^2(t) e^{-\rho t} dt \int_{\mathbb{R}} g^2(x)dx + \chi e^{-\rho T} \int_{\mathbb{R}} R_{y_P}(x,T)g(x)dx, \tag{18}$$

where $\int_{\mathbb{R}} g^2(x)dx$ is known.

According to (18) the policy maker only needs to know the aggregate value of $R_{y_P} g$ at T. Let us define the aggregate variable Z_{y_P} which measures aggregate radiations from y_P along the interior solution as

$$Z_{y_P}(t) = \int_{\mathbb{R}} R_{y_P}(x,t)g(x)dx.$$

We can solve for Z_{y_P} as the following proposition shows:

Proposition 3. *Under Assumption 1, the optimal solution for Z_{y_P} is*

$$Z_{y_P}(t) = e^{(d_1h_1+d_2+d_3h_3)t}\left(Z_{y_P}(0) + \int_0^t M_{y_P}(s)e^{-(d_1h_1+d_2+d_3h_3)s}ds\right),$$

where $Z_{y_P}(0) = \int_{\mathbb{R}} R_{y_P,0}(x,t)g(x)dx$ is known,

$$M_{y_P}(t) = S(y_P,t) - \frac{1}{2}S^2(y_P,t)f(t)\int_{\mathbb{R}} g^2(x)dx \tag{19}$$

and f is defined in Proposition 2.

Proof. See Appendix 7.4. ■

The following corollary studies the two corner solutions at the aggregate associated to the solutions $\theta \equiv 0$ and $\theta \equiv 1$, which provide us with upper and lower bounds for total weighted radiations $Z_{y_P}(t)$ emanating from y_P at time t. Since $Z_{y_P}(0)$ does not depend on y_P, let us write in the following $Z_0 = Z_{y_P}(0)$.

Corollary 2. *Under Theorem 1's assumptions, if there is no effort to contain radiations in neither location, i.e. $\theta(x,t) = 0\ \forall x \in \mathbb{R}$, $\forall t \in [0,T]$, then aggregate radiations, $Z^m_{y_P}$, are given by*

$$Z_{y_P}(t) = e^{(d_1h_1+d_2+d_3h_3)t}\left(Z_0 + \int_0^t S(y_P,s)e^{-(d_1h_1+d_2+d_3h_3)s}ds\right). \tag{20}$$

Note that $Z^m_{y_P}$ is an upper bound for total radiations.

If on the contrary, effort is maximal at all locations, that is, $\theta(x,t) = 1\ \forall x \in \mathbb{R}$, $\forall t \in [0,T]$, then total aggregated radiations grow at a constant rate $d_1h_1 + d_2 + d_3h_3$, that is

$$Z_{y_P}(t) = e^{(d_1h_1+d_2+d_3h_3)t}Z_0, \tag{21}$$

which represents a lower bound for Z_{y_P}.

Proof. See Appendix 7.7. ■

Gathering our results in Propositions 2 and 3, we can write the objective function of the policy maker as

$$\begin{aligned} J(y_P) &= \frac{\chi^2}{4}\int_0^T g^2(x)S^2(y_P,t)e^{2(d_1h_1+d_2+d_3h_3-\rho)(T-t)}dt \\ &+ \chi e^{(d_1h_1+d_2+d_3h_3-\rho)T}\left(Z_0 + \int_0^t M_{y_P}(s)e^{-(d_1h_1+d_2+d_3h_3)s}ds\right) \end{aligned} \tag{22}$$

5.2 Step 2. The optimal location

Next, let us solve the second step problem, namely to choose the location that will maximize overall welfare as defined in (13) by substituting $J(y_P)$ using (22). Decisions are constraint to (14), which can be simplified using Proposition 3. The following proposition provides the optimal location of a nuclear plant when radiations decay with time at a constant rate.

Proposition 4. *Let us assume that $S(y_P,t) = S(y_P)e^{-\eta t}$, with $\eta \in \mathbb{R}^+$ and let us define the location mean value, $\bar{y}$, as $\bar{y} = \int_\Omega y_i dF(i)$. The choice of the optimal location to install a plant depends on the diffusion parameters as well as on the emissions function. The policy maker chooses y^*_P that maximizes (13), where*

$$J(y_P) = -a_1S^2(y_P)v_1(T) + \chi e^{(d_1h_1+d_2+d_3h_3-\rho)T}Z_0 + \chi S(y_P)v_2(T)$$

subject to (14). If $S(y_P)$ is differentiable, $S \in \mathcal{C}^1(\Omega)$, then the optimal location of a nuclear plant, y^*_P, is solution to

$$y^*_P = \bar{y} + \frac{\alpha_2}{2\alpha_1}S'(y^*_P)\left[v_2(T) - 2a_1S(y^*_P)v_1(T)\right] \tag{23}$$

if y_P^* belongs to Ω, (14) holds and the second order condition

$$\frac{\alpha_2}{2\alpha_1} S'(y_P^*) \left[v_2(T) - \frac{\chi}{2} S(y_P^*) v_1(T) \right] > 0$$

also holds. Here

$$\begin{aligned} v_1(T) &= \frac{e^{2(d_1 h_1 + d_2 + d_3 h_3 - \rho)T}}{2(d_1 h_1 + d_2 + d_3 h_3 + \eta) - \rho} \left\{ 1 - e^{[-2(d_1 h_1 + d_2 + d_3 h_3 + \eta) + \rho]T} \right\}, \\ v_2(T) &= e^{(d_1 h_1 + d_2 + d_3 h_3 - \rho)T} \frac{1 - e^{-(d_1 h_1 + d_2 + d_3 h_3 + \eta)T}}{d_1 h_1 + d_2 + d_3 h_3 + \eta}, \\ a_1 &= \frac{\chi^2}{4} \int_{\mathbb{R}} g^2(x) dx. \end{aligned}$$

There is not a unique solution to the policy maker problem if

$$\bar{R} < \int_{\mathbb{R}} R_{y_P}(x, T) g(x) dx,$$

for all $y_P \in \Omega$.

Proof. See Appendix 7.6. ■

Proposition 4 shows that the optimal location choice is not necessarily unique, and that it depends on the time horizon. The following corollary shows the (interior) choices for y_P^* when the time horizon tends to infinite depending on the emissions function S. Since Ω is a compact set in $\mathbb{R}$, let us assume for simplicity that $\Omega = [\underline{Y}, \bar{Y}]$.

Corollary 3. *Under Proposition 4 assumptions and assuming that (14) holds for a compact subset of Ω:*

1. *If $S'(y) = 0$ for all $y \in \Omega$, then $y_p^* = \bar{y}$.*
2. *If diffusion is relatively low, $\frac{\rho}{2} - \eta < d_1 h_1 + d_2 + d_3 h_3 < \rho$, then $\lim_{T \to \infty} y_p^* = \bar{y}$.*
3. *On the contrary, if diffusion is relatively high, meaning here that*

$$d_1 h_1 + d_2 + d_3 h_3 > \rho,$$

then we can distinguish two sub-cases when $S(y_P)$ is monotone:

3.i) If $S'(y_P) > 0$ for all y_P then $\lim_{T \to \infty} y_p^* = \underline{Y}$

3.i) If $S'(y_P) < 0$ for all y_P then $\lim_{T \to \infty} y_p^* = \bar{Y}$.

That is, the policy maker will locate the plant at the location with the lowest emissions, but only if the time horizon is sufficiently large.

Point 1 in the previous corollary shows that if all locations diffuse radiations equally, then the optimal location is spatial mean, independently of the policy maker's eventual spatial preferences and the diffusion characteristics.

6 Conclusions

The recent energetic crisis has revitalized the debate around the need to generate clean and fossil-free energy. Nuclear energy still represents one of the most important non-fossil sources of energy. Several countries have recently revamped their projects to build new nuclear power plants. At the moment, there are several active reactors worldwide, and 60 more new plants will be constructed in the next 10 years. More than in the past, it is crucial to guarantee safety—in particular when a plant is near to a population center—and, at the same time, minimize the management cost. Our paper contributes to

this stream of research. We propose a two steps time-space optimal control model: at the first step, the decision maker wishes to determine the optimal cost by minimizing the weighted combination of radiation and the spatial average level of radiations at the final horizon. In the second step, instead, the decision maker wishes to determine the optimal nuclear power plant location in terms of cost and distance from population centers. If certain assumptions on the functional form of the source function hold, it is possible to determine an optimal closed form solution for the optimal cost in the first step and use it to determine the optimal location y_p at step two. The model provides a useful tool to policy makers to determine the best nuclear power plant location by keeping into considerations containment costs, health cost related to the treatment of contaminated people, and distance from population centers.

References

[AEM+15] Abubakar Sadiq Aliyu, Nikolaos Evangeliou, Timothy Alexander Mousseau, Junwen Wu, and Ahmad Termizi Ramli. An overview of current knowledge concerning the health and environmental consequences of the fukushima daiichi nuclear power plant (fdnpp) accident. *Environment international*, 85:213–228, 2015.

[AUY23] Ali Utku Akar, Mevlut Uyan, and Sukran Yalpir. Spatial evaluation of the nuclear power plant installation based on energy demand for sustainable energy policy. *Environment, Development and Sustainability*, pages 1–36, 2023.

[BBG+20] N.A. Beresford, C.L. Barnett, S. Gashchak, A. Maksimenko, E. Guliaichenko, M.D. Wood, and M. Izquierdo. Radionuclide transfer to wildlife at a 'reference site' in the chernobyl exclusion zone and resultant radiation exposures. *Journal of Environmental Radioactivity*, 211:105661, 2020.

[BGB+09] Barnett, C. L., Gaschak, S., Beresford, N. A., Howard, B. J., and Maksimenko, A. Radionuclide activity concentrations in two species of reptiles from the chernobyl exclusion zone. *Radioprotection*, 44(5):537–542, 2009.

[Cut12] Jerry M Cuttler. Commentary on the appropriate radiation level for evacuations. *Dose-response*, 10(4):473–479, 2012.

[DM17] Richard Denning and Vinod Mubayi. Insights into the societal risk of nuclear power plant accidents. *Risk analysis*, 37(1):160–172, 2017.

[Eng20] John-Oliver Engler. Global and regional probabilities of major nuclear reactor accidents. *Journal of environmental management*, 269:110780, 2020.

[FC18] Ludwig E Feinendegen and Jerry M Cuttler. Biological effects from low doses and dose rates of ionizing radiation: science in the service of protecting humans, a synopsis. *Health physics*, 114(6):623–626, 2018.

[FGMF12] Theodor M Fliedner, Dieter H Graessle, Viktor Meineke, and Ludwig E Feinendegen. Hemopoietic response to low dose-rates of ionizing radiation shows stem cell tolerance and adaptation. *Dose-Response*, 10(4):644–63, 2012.

[HOM+16] Arifumi Hasegawa, Tetsuya Ohira, Masaharu Maeda, Seiji Yasumura, and Koichi Tanigawa. Emergency responses and health consequences after the fukushima accident; evacuation and relocation. *Clinical Oncology*, 28(4):237–244, 2016.

[IAE15] IAEA. *Site survey and site selection for nuclear installations. IAEA safety standard series n° SSG-35.* Vienna: IAEA, 2015.

[K+11] Andreas Kirsch et al. *An introduction to the mathematical theory of inverse problems*, volume 120. Springer, 2011.

[KE07] Son H Kim and James A Edmonds. The challenges and potential of nuclear energy for addressing climate change. Technical report, Pacific Northwest National Lab.(PNNL), Richland, WA (United States), 2007.

[KKK13] Younghwan Kim, Minki Kim, and Wonjoon Kim. Effect of the fukushima nuclear disaster on global public acceptance of nuclear energy. *Energy policy*, 61:822–828, 2013.

[KLZ+17] V. Kashparov, S. Levchuk, M. Zhurba, V. Protsak, Y. Khomutinin, N. A. Beresford, and J. S. Chaplow. Spatial datasets of radionuclide contamination in the ukrainian chernobyl exclusion zone. *NERC Environmental Information Data Centre*, 2017.

[KLZ+18] V. Kashparov, S. Levchuk, M. Zhurba, V. Protsak, Y. Khomutinin, N. A. Beresford, and J. S. Chaplow. Spatial datasets of radionuclide contamination in the ukrainian chernobyl exclusion zone. *Earth System Science Data*, 10(1):339–353, 2018.

[KLZ+20] V. Kashparov, S. Levchuk, M. Zhurba, V. Protsak, N. A. Beresford, and J. S. Chaplow. Spatial radionuclide deposition data from the 60 km radial area around the chernobyl nuclear power plant: results from a sampling survey in 1987. *Earth System Science Data*, 12(3):1861–1875, 2020.

[KYS14] Yang-Hyun Koo, Yong-Sik Yang, and Kun-Woo Song. Radioactivity release from the fukushima accident and its consequences: A review. *Progress in Nuclear Energy*, 74:61–70, 2014.

[Lie] GM Lieberman. Second order parabolic differential equations (1996)(river edge, nj.

[LKL12] Jos Lelieveld, Daniel Kunkel, and Mark G Lawrence. Global risk of radioactive fallout after major nuclear reactor accidents. *Atmospheric Chemistry and Physics*, 12(9):4245–4258, 2012.

[MAC+17] Angela R McLean, Ella K Adlen, Elisabeth Cardis, Alex Elliott, Dudley T Goodhead, Mats Harms-Ringdahl, Jolyon H Hendry, Peter Hoskin, Penny A Jeggo, David JC Mackay, et al. A restatement of the natural science evidence base concerning the health effects of low-level ionizing radiation. *Proceedings of the Royal Society B: Biological Sciences*, 284(1862):20171070, 2017.

[MOT+15] Michio Murakami, Kyoko Ono, Masaharu Tsubokura, Shuhei Nomura, Tomoyoshi Oikawa, Tosihiro Oka, Masahiro Kami, and Taikan Oki. Was the risk from nursing-home evacuation after the fukushima accident higher than the radiation risk? *PLoS one*, 10(9):e0137906, 2015.

[Mub95] Vinod Mubayi. Cost tradeoffs in consequence management at nuclear power plants: A risk based approach to setting optimal long-term interdiction limits for regulatory analyses. Technical report, Brookhaven National Lab, 1995.

[MY21] Vinod Mubayi and Robert Youngblood. Reevaluating the current us nuclear regulatory commission's safety goals. *Nuclear Technology*, 207(3):406–412, 2021.

[NUV21] Matthew Neidell, Shinsuke Uchida, and Marcella Veronesi. The unintended effects from halting nuclear power production: Evidence from fukushima daiichi accident. *Journal of Health Economics*, 79:102507, 2021.

[Pet20] Gianni Petrangeli. *Nuclear safety. Second edition.* Oxford: Butterworth-Heinemann, 2020.

[PW12] Murray H Protter and Hans F Weinberger. *Maximum principles in differential equations.* Springer Science & Business Media, 2012.

[RS16] Thomas Rose and Trevor Sweeting. How safe is nuclear power? a statistical study suggests less than expected. *Bulletin of the Atomic Scientists*, 72(2):112–115, 2016.

[SMS16] Bill Sacks, Gregory Meyerson, and Jeffry A Siegel. Epidemiology without biology: false paradigms, unfounded assumptions, and specious statistics in radiation science (with commentaries by inge schmitz-feuerhake and christopher busby and a reply by the authors). *Biological theory*, 11:69–101, 2016.

[Tik63] Andrei N Tikhonov. Solution of incorrectly formulated problems and the regularization method. *Sov Dok*, 4:1035–1038, 1963.

[TS16] GA Thomas and P Symonds. Radiation exposure and health effects–is it time to reassess the real consequences?, 2016.

[UNS22] UNSCEAR. *Levels and effects of radiation exposure due to the accident at the Fukushima Daiichi Nuclear Power Station: implications of information published since the UNSCEAR 2013 Report (scientific annex B).* New York: United Nations, 2022.

[Vog02] Curtis R Vogel. *Computational methods for inverse problems.* SIAM, 2002.

7 Appendix

7.1 Proof of Proposition 1

The solution to the above ordinary differential equation in t can be easily calculated by means of the following formula:

$$\begin{aligned}
\bar{R}_{y_P}(t) &= e^{(d_2+d_3)t}\left[\int_0^t (1-\bar{\theta}(s))S(y_p,s)e^{-(d_2+d_3)s}ds + \bar{R}_{y_P}(0)\right] && (24)\\
&\leq e^{(d_2+d_3)t}\left[M\int_0^t e^{-(d_2+d_3)s}ds + \bar{R}_{y_P}(0)\right] && (25)\\
&\leq e^{(d_2+d_3)t}\left[\frac{M}{d_2+d_3}(1-e^{-(d_2+d_3)t}) + \bar{R}_{y_P}(0)\right] && (26)\\
&= e^{(d_2+d_3)t}\left(\frac{M}{d_2+d_3} + \bar{R}_{y_P}(0)\right) - \frac{M}{d_2+d_3} && (27)
\end{aligned}$$

7.2 Proof of Theorem 1

If we solve the problem applying Ekelands's method of variation, then we need to define the value function V associated to our problem as

$$V(\theta,R,\lambda_1,\lambda_2,\lambda_3,\lambda_4) = \int_0^T\int_{\mathbb{R}} \theta^2(x,t)e^{-\rho t}dxdt + \phi e^{-\rho T}\int_R R_{y_P}(x,T)g(x)dx$$

$$+\int_0^T\int_{\mathbb{R}} \lambda_1(x,t)\left(-\frac{\partial R_{y_P}(x,t)}{\partial t} + d_1\frac{\partial^2 R_{y_P}(x,t)}{\partial x^2} + d_2R_{y_P}(x,t) + d_3\int_{\mathbb{R}}\phi(x-\omega)R_{y_P}(\omega,t)d\omega + [1-\theta(x,t)]S(y_P,t)\right)dxdt$$

$$+\int_0^T\int_{\mathbb{R}}\lambda_2(x,t)\theta(x,T)dxdt + \int_0^T\int_{\mathbb{R}}\lambda_3(x,t)[1-\theta(x,T)]dxdt + \int_0^T\int_{\mathbb{R}}\lambda_4(x,t)R_{y_P}(x,T)dxdt.$$

Before delving into the minimization problem itself, let us re-arrange some parts of the integrals above. Namely

$$\int_0^T\int_{\mathbb{R}}\lambda_1(x,t)\frac{\partial R_{y_P}(x,t)}{\partial t}dxdt = \int_{\mathbb{R}}\lambda_1(x,t)R_{y_P}(x,t)\mid_0^T - \int_0^T\int_{\mathbb{R}}\frac{\partial\lambda_1(x,t)}{\partial t}(x,t)R_{y_P}(x,t)dxdt.$$

Similarly

$$\int_0^T\int_{\mathbb{R}}\lambda_1(x,t)\frac{\partial^2 R_{y_P}(x,t)}{\partial x^2}dxdt = \int_0^T\lambda_1(x,t)\frac{\partial R_{y_P}(x,t)}{\partial x}\mid_{-\infty}^{\infty}dt - \int_0^T\int_{\mathbb{R}}\frac{\partial\lambda_1(x,t)}{\partial x}\frac{\partial R_{y_P}(x,t)}{\partial x}dxdt$$

$$= -\int_0^T\frac{\partial\lambda_1(x,t)}{\partial x}R_{y_P}(x,t)\mid_{-\infty}^{\infty}dt + \int_0^T\int_{\mathbb{R}}\frac{\partial^2\lambda_1(x,t)}{\partial x^2}R_{y_P}(x,t)dxdt.$$

Then, if we assume that

$$\lim_{x\to\infty}\frac{\partial\lambda_1(x,t)}{\partial x} = 0,$$

we have that

$$V(\theta,R,\lambda_1,\lambda_2,\lambda_3,\lambda_4)=\int_0^T\int_{\mathbb{R}}\theta^2(x,t)e^{-\rho t}dxdt+\chi e^{-\rho T}\int_{\mathbb{R}}R_{y_P}(x,T)g(x)dx$$
$$-\int_{\mathbb{R}}\lambda_1(x,t)R_{y_P}(x,t)\mid_0^T dx+\int_0^T\int_{\mathbb{R}}\frac{\partial\lambda_1(x,t)}{\partial t}(x,t)R_{y_P}(x,t)dxdt$$
$$+\int_0^T\int_{\mathbb{R}}d_1\frac{\partial^2\lambda_1(x,t)}{\partial x^2}R_{y_P}(x,t)dxdt$$
$$+\int_0^T\int_{\mathbb{R}}\lambda_1(x,t)\left(d_2R_{y_P}(x,t)+d_3\int_R\phi(x-\omega)R_{y_P}(\omega,t)d\omega+[1-\theta(x,t)]S(y_P,t)\right)dxdt$$
$$+\int_0^T\int_{\mathbb{R}}\lambda_2(x,t)\theta(x,t)dxdt+\int_0^T\int_{\mathbb{R}}\lambda_3(x,t)[1-\theta(x,t)]dxdt+\int_0^T\int_{\mathbb{R}}\lambda_4(x,t)R_{y_P}(x,t)dxdt.$$

Let us assume that there exists an optimal solution $(\theta^*,R^*_{y_P})$ and that any other feasible trajectory (θ,R_{y_P}) can be written as a deviation from the optimal as the sum of the optimal solution plus another feasible solution (n,r) to the policymaker problem:

$$\begin{aligned}\theta &= \theta^*+\epsilon n,\\ R_{y_P} &= R^*_{y_P}+\epsilon r,\end{aligned}$$

where $\epsilon\in\mathbb{R}$ and $n,s\in C^{2,1}(\mathbb{R}\times(0,T))\cap L(\Omega\times[0,T])$.

Then, V becomes a function of ϵ, the optimal solution and the co-state variables, and we can optimize V with respect to ϵ, the deviation from the optimum. We take the first order condition of V with respect to ϵ:

$$\frac{\partial V(\theta,R,\lambda_1,\lambda_2,\lambda_3,\lambda_4)}{\partial\epsilon}=\int_0^T\int_{\mathbb{R}}2\theta(x,t)n(x,t)e^{-\rho t}dxdt+\chi e^{-\rho T}\int_{\mathbb{R}}r_{y_P}(x,T)g(x)dx$$
$$-\int_{\mathbb{R}}\lambda_1(x,T)r_{y_P}(x,T)dx+\int_0^T\int_{\mathbb{R}}\frac{\partial\lambda_1(x,t)}{\partial t}(x,t)r_{y_P}(x,t)dxdt$$
$$+\int_0^T\int_{\mathbb{R}}d_1\frac{\partial^2\lambda_1(x,t)}{\partial x^2}r_{y_P}(x,t)dxdt$$
$$+\int_0^T\int_{\mathbb{R}}\lambda_1(x,t)\left(d_2r_{y_P}(x,t)+d_3\int_{\mathbb{R}}\phi(x-\omega)r_{y_P}(\omega,t)d\omega+[1-n(x,t)]S(y_P,t)\right)dxdt$$
$$+\int_0^T\int_{\mathbb{R}}\lambda_2(x,t)n(x,t)dxdt+\int_0^T\int_{\mathbb{R}}\lambda_3(x,t)[1-n(x,t)]dxdt+\int_0^T\int_{\mathbb{R}}\lambda_4(x,t)r_{y_P}(x,t)dxdt.$$

It will be useful to note that

$$\int_{\mathbb{R}}\int_{\mathbb{R}}\lambda_1(x,t)\phi(x-\omega)r_{y_P}(\omega,t)d\omega dx=\int_{\mathbb{R}}\int_{\mathbb{R}}\lambda_1(\omega,t)\phi(\omega-x)r_{y_P}(x,t)d\omega dx=\int_{\mathbb{R}}r_{y_P}(x,t)\int_{\mathbb{R}}\lambda_1(\omega,t)\phi(\omega-x)d\omega dx$$

We obtain the following set of necessary optimal conditions:

$$\begin{cases}\lim_{x\to\pm\infty}\frac{\partial\lambda_1(x,t)}{\partial x}=0,\\ \lambda_1(x,T)=\chi e^{-\rho T}g(x),\\ n: \quad 2\theta(x,t)e^{-\rho t}-\lambda_1(x,t)S(y_P,t)+\lambda_2(x,t)-\lambda_3(x,t)=0,\\ r: \quad \frac{\partial\lambda_1(x,t)}{\partial t}+d_1\frac{\partial^2\lambda_1(x,t)}{\partial x^2}+d_2\lambda_1(x,t)+d_3\int_R\phi(\omega-x)\lambda_1(\omega,t)d\omega+\lambda_4(x,t)=0.\end{cases}$$

We can define $\mu_i=e^{\rho t}\lambda_i$ and rewrite the set of constraints as

$$\begin{cases}\lim_{x\to\pm\infty}\frac{\partial\mu_1(x,t)}{\partial x}=0,\\ \mu_1(x,T)=\chi g(x),\\ n: \quad 2\theta(x,t)-\mu_1(x,t)S(y_P,t)+\mu_2(x,t)-\mu_3(x,t)=0,\\ r: \quad \frac{\partial\mu_1(x,t)}{\partial t}+d_1\frac{\partial^2\mu_1(x,t)}{\partial x^2}+(d_2-\rho)\mu_1(x,t)+d_3\int_R\phi(\omega-x)\mu_1(\omega,t)d\omega+\mu_4(x,t)=0.\end{cases}$$

Then, the complete set of optimal conditions is

$$\begin{cases} \frac{\partial R_{y_P}(x,t)}{\partial t} = d_1 \frac{\partial^2 R_{y_P}(x,t)}{\partial x^2} + d_2 R_{y_P}(x,t) + d_3 \int_{\mathbb{R}} \phi(x-\omega) R_{y_P}(\omega,t) d\omega + [1-\theta(x,t)] S(y_P,t), \\ \frac{\partial \mu_1(x,t)}{\partial t} + d_1 \frac{\partial^2 \mu_1(x,t)}{\partial x^2} + (d_2-\rho)\mu_1(x,t) + d_3 \int_{\mathbb{R}} \phi(\omega-x)\mu_1(\omega,t) d\omega + \mu_4(x,t) = 0, \\ 2\theta(x,t) - \mu_1(x,t) S(y_P,t) + \mu_2(x,t) - \mu_3(x,t) = 0, \\ \lim_{x\to\pm\infty} \frac{\partial R_{y_P}(x,t)}{\partial x} = 0, \\ \lim_{x\to\pm\infty} \frac{\partial \mu_1(x,t)}{\partial x} = 0, \\ \mu_i(x,t) \geq 0, \\ \mu_1(x,T) = \chi g(x), \\ \mu_2(x,t)\theta(x,t) = 0, \\ \mu_3(x,t)\left[1-\theta(x,t)\right] = 0, \\ \mu_4(x,t) R_{y_P}(x,t) = 0, \\ R_{y_P}(x,0) = R_0(x), \\ 0 \leq \theta(x,t) \leq 1, \\ R_{y_P}(x,t) \geq 0. \end{cases}$$

Let us now focus our attention to the interior solution, when $0 < \theta(x,t) < 1$. Along the interior solution, and using that in this case

$$2\theta(x,t) = \mu_1(x,t) S(y_P,t)$$

then the optimal interior solution verifies that

$$I \begin{cases} \frac{\partial R_{y_P}(x,t)}{\partial t} = d_1 \frac{\partial^2 R_{y_P}(x,t)}{\partial x^2} + d_2 R_{y_P}(x,t) + d_3 \int_{\mathbb{R}} \phi(x-\omega) R_{y_P}(\omega,t) d\omega + [1 - \frac{1}{2}\mu_1(x,t) S(y_P,t)] S(y_P,t), \\ \frac{\partial \mu_1(x,t)}{\partial t} + d_1 \frac{\partial^2 \mu_1(x,t)}{\partial x^2} + (d_2-\rho)\mu_1(x,t) + d_3 \int_{\mathbb{R}} \phi(\omega-x)\mu_1(\omega,t) d\omega = 0, \\ \lim_{x\to\pm\infty} \frac{\partial R_{y_P}(x,t)}{\partial x} = 0, \\ \lim_{x\to\pm\infty} \frac{\partial \mu_1(x,t)}{\partial x} = 0, \\ \mu_1(x,t) \geq 0, \\ \mu_1(x,T) = \chi g(x), \\ R_{y_P}(x,0) = R_0(x), \\ R_{y_P}(x,t) \geq 0, \end{cases}$$

since along the interior optimal solution, $\mu_2(x,t) = \mu_3(x,t) = \mu_4(x,t) = 0$. Note that the equation for μ_1 can be solved independently of R_{y_P}. The problem for μ_1 is

$$I_{\mu_1} \begin{cases} \frac{\partial \mu_1(x,t)}{\partial t} + d_1 \frac{\partial^2 \mu_1(x,t)}{\partial x^2} + (d_2-\rho)\mu_1(x,t) + d_3 \int_{\mathbb{R}} \phi(\omega-x)\mu_1(\omega,t) d\omega = 0, \\ \lim_{x\to\pm\infty} \frac{\partial \mu_1(x,t)}{\partial x} = 0, \\ \mu_1(x,t) \geq 0, \\ \mu_1(x,T) = \chi g(x), \end{cases}$$

7.3 Proof of Proposition 2

Note that under Assumption 1, the PDE for μ_1 in I_{μ_1} can be rewritten as

$$f_t g + d_1 f g_{xx} + (d_2-\rho) f g + d_3 \int_{\mathbb{R}} \phi(\omega - x) f(t) g(\omega) d\omega = 0,$$

or assuming that $g(x) \neq 0$ for any x, we can divide by $g(x)$ to obtain

$$f_t(t) + d_1 f(t)\frac{g_{xx}(x)}{g(x)} + (d_2 - \rho)f(t) + \frac{d_3 f(t)}{g(x)}\int_{\mathbb{R}} \phi(\omega - x)g(\omega)d\omega = 0.$$

Under Assumption 1, function f solves

$$f_t(t) + (d_1 h_1 + d_2 + d_3 h_3 - \rho)f(t) = 0,$$

with $f(T) = \chi$. It is straightforward to show that function f is

$$f(t) = \chi e^{(d_1 h_1 + d_2 + d_3 h_3 - \rho)(T-t)}.$$

Then,

$$\mu_1(x,t) = \chi g(x) e^{(d_1 h_1 + d_2 + d_3 h_3 - \rho)(T-t)}.$$

7.4 Proof of Proposition 3

Let us start by multiplying the PDE describing the dynamics of R_{y_P} in I by $g(x)$:

$$g(x)\frac{\partial R_{y_P}(x,t)}{\partial t} = d_1 g(x)\frac{\partial^2 R_{y_P}(x,t)}{\partial x^2} + d_2 g(x) R_{y_P}(x,t)$$

$$+d_3 g(x)\int_{\mathbb{R}} \phi(x-\omega)R_{y_P}(\omega,t)d\omega + [1 - \tfrac{1}{2}\mu_1(x,t)S(y_P,t)]g(x)S(y_P,t).$$

Then, let us take the integral of the expression above over $\mathbb{R}$

$$\int_{\mathbb{R}} g(x)\frac{\partial R_{y_P}(x,t)}{\partial t}dx = d_1 \int_{\mathbb{R}} g(x)\frac{\partial^2 R_{y_P}(x,t)}{\partial x^2}dx + d_2 \int_{\mathbb{R}} g(x) R_{y_P}(x,t)dx$$

$$+d_3 \int_{\mathbb{R}} g(x)\int_{\mathbb{R}} \phi(x-\omega)R_{y_P}(\omega,t)d\omega dx + \int_{\mathbb{R}}[1 - \tfrac{1}{2}\mu_1(x,t)S(y_P,t)]g(x)S(y_P,t)dx.$$

Let us analyse term by term. First,

$$\int_{\mathbb{R}} g(x)\frac{\partial R_{y_P}(x,t)}{\partial t} = \frac{\partial}{\partial t}\int_{\mathbb{R}} g(x) R_{y_P}(x,t)dxr = \frac{\partial Z(t)}{\partial t}.$$

Focusing on the second term and using integration by parts

$$\int_{\mathbb{R}} g(x)\frac{\partial^2 R_{y_P}(x,t)}{\partial x^2}dx = g(x)\frac{\partial R_{y_P}(x,t)}{\partial x}\mid_{-\infty}^{\infty} - \int_{\mathbb{R}} g'(x)\frac{\partial R_{y_P}(x,t)}{\partial x}dx$$

$$= -R_{y_P}(x,t)g'(x)\mid_{-\infty}^{\infty} + \int_{\mathbb{R}} g''(x)R_{y_P}(x,t)dx.$$

Hence, under Assumption 1

$$\int_{\mathbb{R}} g(x)\frac{\partial^2 R_{y_P}(x,t)}{\partial x^2}dx = h_1 \int_{\mathbb{R}} g(x)R_{y_P}(x,t)dx = h_1 Z(t)$$

Focusing now on the third term and under Assumption 1

$$\int_{\mathbb{R}} g(x)\phi(x-\omega)dx = h_3 g(\omega).$$

Then

$$\int_{\mathbb{R}}\int_{\mathbb{R}} g(x)\phi(x-\omega)R_{y_P}(\omega,t)d\omega dx = h_3 \int_{\mathbb{R}} g(\omega)R_{y_P}(\omega,t)d\omega dx = h_3 Z(t).$$

Under these assumptions for g, the dynamics of the aggregate variable Z are described by

$$Z_{y_P,t}(t) - (d_1 h_1 + d_2 + d_3 h_3)Z_{y_P}(t) = S(y_P,t)\int_{\mathbb{R}} g(x)dx - \frac{1}{2}S^2(y_P,t)f(t)\int_{\mathbb{R}} g^2(x)dx.$$

Or using that $\int_{\mathbb{R}} g(x)dx = 1$:

$$Z_{y_P,t}(t) - (d_1h_1 + d_2 + d_3h_3)Z_{y_P}(t) = S(y_P,t) - \frac{1}{2}S^2(y_P,t)f(t)\int_{\mathbb{R}} g^2(x)dx. \tag{28}$$

We can denote by $M_{y_P}(t)$ the right hand side of (29) and write

$$Z_{y_P,t}(t) - (d_1h_1 + d_2 + d_3h_3)Z_{y_P}(t) = M_{y_P}(t), \tag{29}$$

with $Z_{y_P}(0)$ known and given by

$$Z_{y_P}(0) = \int_{\mathbb{R}} R_{y_P}(x,0)g(x)dx = \int_{\mathbb{R}} R_0(x)g(x)dx,$$

which is independent of y_P, so that we will write $Z_{y_P}(0) = Z_0$.

Using the standard technique of variation of parameters, we know that the solution Z_{y_P} is given by

$$Z_{y_P}(t) = e^{(d_1h_1+d_2+d_3h_3)t}\left(Z_0 + \int_0^t M_{y_P}(s)e^{-(d_1h_1+d_2+d_3h_3)s}ds\right). \tag{30}$$

Then

$$Z_{y_P}(T) = e^{(d_1h_1+d_2+d_3h_3)T}\Big[Z_0 + \int_0^T S(y_P,v)e^{-(d_1h_1+d_2+d_3h_3)v}dv$$

$$+\tfrac{1}{2}\int_{\mathbb{R}} g^2(x)dx\int_0^T S^2(y_P,v)f(v)e^{-(d_1h_1+d_2+d_3h_3)v}dv,$$

Plugging in $f(t)$ from Proposition 3

$$f(t) = \chi e^{(d_1h_1+d_2+d_3h_3-\rho)(T-t)}.$$

we obtain the result shown in the proposition, that is,

$$Z_{y_P}(T) = e^{(d_1h_1+d_2+d_3h_3)T}Z_0 + e^{(d_1h_1+d_2+d_3h_3)T}\int_0^T S(y_P,v)e^{-(d_1h_1+d_2+d_3h_3)v}dv$$

$$+\tfrac{1}{2}\chi e^{(d_1h_1+d_2+d_3h_3)T}\int_{\mathbb{R}} g^2(x)dx\int_0^T S^2(y_P,v)e^{-2(d_1h_1+d_2+d_3h_3)v}dv.$$

7.5 Proof of corollary 3

We study next the two corner solutions at the aggregate associated to the solutions $\theta(x,t) \equiv 0\ \forall x \in \mathbb{R}$ $\forall t \in [0,T]$ and $\theta(x,t) \equiv 1\ \forall x \in \mathbb{R}\ \forall t \in [0,T]$, which provide us with upper and lower bounds for total weighted radiations $\bar{R}_{y_P}(t)$ emanating from y_P at time t.

1) If $\theta \equiv 0$, then for every $t > 0$, Z_{y_P} satisfies (30) with $M_{y_P}(t) = S(y_P,t)$. Then

$$Z_{y_P}(t) = e^{(d_1h_1+d_2+d_3h_3)t}\left(Z_0 + \int_0^t S(y_P,s)e^{-(d_1h_1+d_2+d_3h_3)s}ds\right).$$

2) If $\theta \equiv 1$, then $\bar{R}_{y_P}(t)$ satisfies (30) with $M_{y_P}(t) = 0$. In this case

$$Z_{y_P}(t) = e^{(d_1h_1+d_2+d_3h_3)t}Z_0.$$

7.6 Proof of Proposition 4

.

$$\begin{aligned} J(y_P) &= \frac{\chi^2}{4}\int_0^T g^2(x)S^2(y_P,t)e^{2(d_1h_1+d_2+d_3h_3-\rho)(T-t)}dt \\ &+ \chi e^{(d_1h_1+d_2+d_3h_3-\rho)T}\left(Z_0 + \int_0^t M_{y_P}(s)e^{-(d_1h_1+d_2+d_3h_3)s}ds\right) \end{aligned}$$

Substituting M_{y_P} using (19)

$$\begin{aligned} J(y_P) &= \frac{\chi^2}{4}\int_0^T\int_{\mathbb{R}} g^2(x)S^2(y_P,t)e^{2(d_1h_1+d_2+d_3h_3-\rho)(T-t)}dt \\ &+ \chi e^{(d_1h_1+d_2+d_3h_3-\rho)T}Z_0 \\ &+ \chi e^{(d_1h_1+d_2+d_3h_3-\rho)T}\int_0^t S(y_P,t)e^{-(d_1h_1+d_2+d_3h_3)s}ds \\ &- \frac{\chi}{2}e^{(d_1h_1+d_2+d_3h_3-\rho)T}\int_{\mathbb{R}} g^2(x)dx\int_0^t S^2(y_P,t)f(s)e^{-(d_1h_1+d_2+d_3h_3)s}ds. \end{aligned}$$

Let us assume that $S(y_P,t) = S(y_P)e^{-\eta t}$, with $\eta \in \mathbb{R}^+$. After substituting for f and after some computations we obtain that

$$\begin{aligned} J(y_P) &= \frac{-\chi^2}{4}S^2(y_P)\frac{e^{2(d_1h_1+d_2+d_3h_3-\rho)T}}{2(d_1h_1+d_2+d_3h_3+\eta)-\rho}\left\{1-e^{[-2(d_1h_1+d_2+d_3h_3+\eta)+\rho]T}\right\}\int_{\mathbb{R}} g^2(x)dx \\ &+ \chi e^{(d_1h_1+d_2+d_3h_3-\rho)T}Z_0 \\ &+ \chi e^{(d_1h_1+d_2+d_3h_3-\rho)T}S(y_P)\frac{1-e^{-(d_1h_1+d_2+d_3h_3+\eta)T}}{d_1h_1+d_2+d_3h_3+\eta}. \end{aligned}$$

For simplicity reasons, let us denote by

$$\begin{aligned} v_1(T) &= \frac{e^{2(d_1h_1+d_2+d_3h_3-\rho)T}}{2(d_1h_1+d_2+d_3h_3+\eta)-\rho}\left\{1-e^{[-2(d_1h_1+d_2+d_3h_3+\eta)+\rho]T}\right\}, \\ v_2(T) &= e^{(d_1h_1+d_2+d_3h_3-\rho)T}\frac{1-e^{-(d_1h_1+d_2+d_3h_3+\eta)T}}{d_1h_1+d_2+d_3h_3+\eta}, \\ a_1 &= \frac{\chi^2}{4}\int_{\mathbb{R}} g^2(x)dx. \end{aligned}$$

Then we can write that

$$J(y_P) = -a_1S^2(y_P)v_1(T) + \chi e^{(d_1h_1+d_2+d_3h_3-\rho)T}Z_0 + \chi S(y_P)v_2(T),$$

The policy maker wishes to maximize (13) subject to (14), so that under the assumptions on differentiability in this proposition, we can construct the associated Lagrangian:

$$L(y_P,\lambda) = \alpha_1\int_\Omega (y_P-y_i)^2dF(i) - \alpha_2J(y_P) + \lambda\left(\bar{R} - \int_{\mathbb{R}} R_{y_P}(x,T)g(x)dx\right).$$

Taking the first order condition with respect to $y_p \in \Omega$ we obtain that y_P^* is implicitly defined as the solution to

$$2\alpha_1y_P^*\int_\Omega dF(i) - 2\alpha_1\int_\Omega y_idF(i) - \alpha_2J'(y_P^*) - \lambda\int_\Omega \frac{\partial}{\partial y_P}R_{y_P}(x,T)g(x)dx = 0,$$

with

$$\lambda\left(\bar{R} - \int_{\mathbb{R}} R_{y_P}(x,T)g(x)dx\right) = 0.$$

Since $\int_\Omega dF(i) = 1$ and defining $\bar{y}$ as $\bar{y} = \int_\Omega y_i dF(i)$, we obtain that there exists an interior solution y_P^* defined as

$$y_P^* = \bar{y} + \frac{\alpha_2}{2\alpha_1} S'(y_P^*) \left[v_2(T) - 2a_1 S(y_P^*) v_1(T) \right], \tag{31}$$

$$\bar{R} > \int_{\mathbb{R}} R_{y_P}(x,T) g(x) dx. \tag{32}$$

There is not a unique solution to the policy maker problem if

$$\bar{R} < \int_{\mathbb{R}} R_{y_P}(x,T) g(x) dx,$$

for all y_P.

7.7 Proof of Corollary 3

.

From (31) it is straightforward that if the emissions function is constant, that is if $S'(y) = 0$ for all y, then $y_P^* = \bar{y}$.

If $S'(y) \neq 0$, then we can distinguish two cases:

1. If $\frac{\rho}{2} - \eta < d_1 h_1 + d_2 + d_3 h_3 < \rho$, then $\lim_{T\to\infty} v_1(T) = \lim_{T\to\infty} v_2(T) = 0$, so that $\lim_{T\to\infty} y_p^* = \bar{y}$.
2. If $d_1 h_1 + d_2 + d_3 h_3 > \rho$, then we can write (31) as follows

$$y_P^* = \bar{y} + \frac{\alpha_2}{2\alpha_1} S'(y_P^*) e^{2(d_1 h_1 + d_2 + d_3 h_3 - \rho)T} \left[\tilde{v}_2(T) - 2a_1 S(y_P^*) \tilde{v}_1(T) \right],$$

where

$$\tilde{v}_1(T) = \frac{1}{2(d_1 h_1 + d_2 + d_3 h_3 + \eta) - \rho} \left\{ 1 - e^{[-2(d_1 h_1 + d_2 + d_3 h_3 + \eta) + \rho]T} \right\},$$

$$\tilde{v}_2(T) = e^{-(d_1 h_1 + d_2 + d_3 h_3 - \rho)T} \frac{1 - e^{-(d_1 h_1 + d_2 + d_3 h_3 + \eta)T}}{d_1 h_1 + d_2 + d_3 h_3 + \eta}.$$

Note that $\lim_{T\to\infty} \tilde{v}_1(T) > 0$ and $\lim_{T\to\infty} \tilde{v}_2(T) = 0$. We can distinguish two sub-cases when $S(y_P)$ is monotone:

2.i) If $S'(y_P) > 0$ for all y_P then $\lim_{T\to\infty} y_p = \underline{Y}$

2.i) If $S'(y_P) < 0$ for all y_P then $\lim_{T\to\infty} y_p = \bar{Y}$.